Eulerian and Lagrangian statistics in an exactly solvable turbulent shear model with a random background mean

Cite as: Phys. Fluids **31**, 105115 (2019); https://doi.org/10.1063/1.5121705
Submitted: 09 August 2019 . Accepted: 28 September 2019 . Published Online: 28 October 2019

Mustafa A. Mohamad, and Andrew J. Majda

Physics of Fluids ARTICLE scitation.org/journal/phf

Eulerian and Lagrangian statistics in an exactly solvable turbulent shear model with a random background mean

Cite as: Phys. Fluids 31, 105115 (2019); doi: 10.1063/1.5121705
Submitted: 9 August 2019 • Accepted: 28 September 2019 •
Published Online: 28 October 2019

Mustafa A. Mohamad[a] and Andrew J. Majda[a]

AFFILIATIONS

Courant Institute of Mathematical Sciences, 251 Mercer Street, New York, New York 10012, USA

[a]mmus@nyu.edu and jonjon@cims.nyu.edu

ABSTRACT

We study the Lagrangian statistics of passively advected particles in an elementary velocity model for turbulent shear. The stochastic velocity model is exactly solvable and includes features that highlight the important differences between Lagrangian and Eulerian velocity statistics, which are not equal in the present context. A major element of the velocity model is the presence of a random, spatially uniform background mean, which is superimposed on a turbulent shear with a spectrum that typically follows a power law. We directly solve for the Eulerian and Lagrangian statistics and show how the sweeping motion of the background mean affects the Lagrangian velocity statistics with faster decaying correlations that oscillate more rapidly compared to the Eulerian velocity. This arises due to interaction of the cross-sweeps of the mean flow with the shear component, which determines Lagrangian tracer transport rates. We derive explicit expressions for the tracer dispersion that demonstrate how the dispersion rate depends on model parameters. We validate the predictions with numerical experiments in various test regimes that also highlight the behavior of Lagrangian particles in space. The proposed exactly solvable model serves as a test problem for Eulerian spectral recovery via Lagrangian data assimilation and parameter estimation methods.

I. INTRODUCTION

We study the statistics of passive tracers advected by turbulent stochastic velocity fields. Lagrangian tracers or drifters are massless particles that passively move throughout a flow field. Examples include physical tracers, such as temperature, and chemical tracers, including solute concentration, and idealized measurement devices such as sensors used to measure various physical quantities. Indeed, Lagrangian drifters serve as an important source for atmospheric and oceanographic measurements.[1,2] Models based on the Lagrangian perspective are commonly used to study pollution transport and air quality,[3] turbulent combustion,[4,5] turbulent entrainment processes,[6] particle aggregation, and turbulence,[7,8] in part due to the conceptual simplicity of the viewpoint and its connection with the physics of mixing and dispersion.[9] A key problem for any Lagrangian model is to understand the effects of the flow field on the statistical (ensemble) properties of the particles.

We propose here an elementary turbulent velocity model, consisting of a random shear and a random spatially uniform mean. The velocity model is exactly solvable and is used to highlight the differences between Eulerian and Lagrangian velocity statistics, which are not equivalent in the current context. We derive explicit equations for the Eulerian and Lagrangian velocity correlation functions and the mean-square tracer displacement in the short and long time limits. We demonstrate how various features of the model interact to determine particle behavior. In particular, we discuss the important interplay between the mean and the shear component of the velocity model in determining tracer transport and mixing properties. We explicitly show how the sweeping motion of the background mean affects the Lagrangian velocity statistics with faster decaying correlations that oscillate more rapidly compared to the Eulerian velocity. This fact has important implications for the spectral recovery problem since the Fourier transform of the velocity correlation gives the kinetic energy spectrum.[10] There is a rich range of model regimes that determine particle behavior and mixing rates, which we explain

and demonstrate by appealing to both numerical simulations and theory.

The Lagrangian characterization of diffusion processes and their statistics has been studied in various contexts over the years. The seminal paper by Taylor[11] studied diffusion due to the continuous motion of particles. The characterization and modeling of both single-particle and multiparticle (pairs or groups) dispersion statistics, including data from observations, was later expanded upon and summarized in important works by Batchelor,[12,13] Richardson,[14] and others in Refs. 15–19. As mentioned, it is conceptually more natural to view turbulent mixing in the Lagrangian frame, and more recent works on turbulent mixing include Refs. 20–24, which investigate and characterize particle dispersion in turbulent flows and develop simplified Lagrangian models in turbulent flows via various approaches. This statistical characterization of Lagrangian motions is indeed crucial since Lagrangian instruments are a dominant data collection method in studying the environment, especially the atmosphere and ocean, since they can cover large distances and explore large spatial regions compared to more costly fixed Eulerian measurement devices.[1] In recent studies, Lagrangian observational data from surface drifters and floats in the ocean have been used to study various properties of the ocean including, e.g., the kinetic energy spectrum and pair dispersion statistics in the Gulf of Mexico[25,26] and to construct eddy diffusivity approximations of the global map.[27]

Complementary to the Lagrangian viewpoint, the Eulerian characterization and study of turbulent diffusion and mixing has its own significance.[28–30] The report[30] studied simple mathematical models for turbulent diffusion of passive scalar fields, which connect and explain anomalous diffusion in random velocity field models. The Eulerian perspective for passive scalar statistics in random shear flows with mean sweeps was also carried out in a different context in Refs. 31 and 32. Despite the simplicity of such simplified passive scalar turbulence models, they capture and preserve key features in various inertial range statistics for turbulent diffusion, including intermittency and extreme events,[31,33] and serve as important paradigm models.

Our approach studies the Lagrangian statistics of a random turbulent shear model with a random background mean. The combined velocity and tracer model has a special conditionally Gaussian structure[34,35] (conditional on observed tracer trajectories, the combined model is Gaussian). Despite the Gaussian velocity field structure, the tracer dynamics remain nonlinear with non-Gaussian statistics since the Lagrangian observations are coupled nonlinearly to the velocity field. The exactly solvable nature of the proposed model makes it suitable as a benchmark problem for Lagrangian data assimilation and parameter estimation methods,[36–39] including spectral recovery of the turbulent Eulerian velocity field and other uncertainty quantification problems. Filtering such conditionally Gaussian models for Lagrangian data assimilation has been explored in Refs. 40 and 41; in particular, Ref. 41 developed mathematical guidelines and information theoretical limits on recovery, and in Ref. 40, the spectral recovery performance and filter approximations are studied. The intuition and analysis we conduct here on the simplified shear model, in particular, the effects of the interaction between the shear structure and the background mean in the velocity field, provides guidelines for further work on the estimation and spectral recovery problem. This can help in interpreting when spectral recovery is an attainable goal and when recovery performance is expected to be poor. More specifically, shorter correlations in the Lagrangian frame relative to the Eulerian field are expected to lead to worse recovery of the kinetic energy spectrum, due to the information loss induced due to turbulence mixing. The relation between the two correlation functions in the different reference frames is explained and related to the parameters of the simplified fluid shear model.

A. Outline

In Sec. II, we provide an overview of Lagrangian and Eulerian statistics. The general velocity model is described in Sec. III and the aligned shear test model in Sec. IV. The Eulerian statistics for the aligned shear model are discussed in Sec. V. The Lagrangian statistics, including the mean Lagrangian velocity and Lagrangian velocity fluctuations, are then derived in Sec. VI; the final result for the Lagrangian correlation function is given in Sec. VI D. We discuss the differences between the Eulerian and Lagrangian velocity correlation functions in Sec. VI D. In Sec. VIII, we derive results for the mixing rate in various regimes and discuss mixing properties in terms of model parameters. Numerical simulations and regime studies are presented in Sec. IX. Concluding remarks are made in Sec. X. Nomenclature used throughout the work is provided in Appendix A.

II. OVERVIEW ON TURBULENT DIFFUSION AND LAGRANGIAN AND EULERIAN QUANTITIES

The transport of a passive scalar $T(\boldsymbol{x},t)$ is governed by the advection-diffusion equation

$$\frac{\partial T(\boldsymbol{x},t)}{\partial t} + \boldsymbol{v}(\boldsymbol{x},t)\cdot\nabla T(\boldsymbol{x},t) = \kappa\Delta T(\boldsymbol{x},t) + f(\boldsymbol{x},t), \qquad \nabla\cdot\boldsymbol{v}(\boldsymbol{x},t) = 0, \tag{1}$$

where $\kappa > 0$ is the molecular diffusivity constant, $\boldsymbol{v}(\boldsymbol{x},t)$ is an incompressible velocity field satisfying $\nabla\cdot\boldsymbol{v} = 0$, and $f(\boldsymbol{x},t)$ is a source term. In this article, we focus on the statistical aspects of Lagrangian particles advected by idealized velocity fields. In general, $\boldsymbol{v}$ is the solution of the Navier-Stokes equation. However, it is difficult to make progress on exact solutions and in understanding how various flow features interact to determine tracer transport, following the direct numerical simulation approach. We instead consider idealized *random* fluid flows, which retain important qualitative features of true flows, where the random realizations of the idealized velocity field are designed to mimic the complex spatiotemporal patterns of real turbulent flows.

We discuss some elementary facts regarding Eulerian and Lagrangian velocity fields and the motion of tracer particles. For simplicity, in this section, we consider tracer particles under pure advection ($\kappa = 0$), but later include molecular diffusivity with $\kappa > 0$. The Eulerian velocity field is described in terms of a fixed system of space-time coordinates $\boldsymbol{v}(\boldsymbol{x},t)$, which denotes the velocity of a fluid at position $\boldsymbol{x}$ and time t. In the Lagrangian description, we mark or label particles at time zero by their initial spatial coordinate $\boldsymbol{\alpha}$. The position at later times of a tracer particle, initially marked $\boldsymbol{\alpha}$ at $t = 0$,

is given by its trajectory $\boldsymbol{X}(\boldsymbol{\alpha}, t)$ function, which satisfies

$$\frac{d\boldsymbol{X}(\boldsymbol{\alpha},t)}{dt} = \boldsymbol{v}(\boldsymbol{X}(\boldsymbol{\alpha},t),t), \qquad \boldsymbol{X}(\boldsymbol{\alpha},0) = \boldsymbol{\alpha}. \tag{2}$$

The Lagrangian velocity is defined by the velocity of the particle labeled by $\boldsymbol{\alpha}$ at time t and is related to the Eulerian velocity field as follows:

$$\boldsymbol{v}^{\mathsf{L}}(\boldsymbol{\alpha},t) \equiv \boldsymbol{v}(\boldsymbol{X}(\boldsymbol{\alpha},t),t). \tag{3}$$

In principle, if the Lagrangian velocity field is known, we can directly obtain the particle trajectories by

$$\boldsymbol{X}(\boldsymbol{\alpha},t) = \boldsymbol{\alpha} + \int_0^t \boldsymbol{v}^{\mathsf{L}}(\boldsymbol{\alpha},s)\,ds. \tag{4}$$

However, this is usually not possible since determining the Lagrangian velocity from the Eulerian velocity itself requires knowledge of tracer particle trajectories. It is easy to see why the Eulerian and Lagrangian velocity will not, in general, be equivalent for a variety of flows. The presence of a spatially dependent mean flow, for example, would immediately lead to differences between the two quantities.

A. Overview on Eulerian and Lagrangian velocity statistics

In general, we consider velocity models with a mean, so we separate the randomly fluctuating component of the Eulerian and Lagrangian velocities from their statistical (ensemble) mean, $\boldsymbol{v} = \overline{\boldsymbol{v}} + \widetilde{\boldsymbol{v}}$, where $\overline{\boldsymbol{v}} = \langle \boldsymbol{v} \rangle$, and similarly for the Lagrangian velocity $\boldsymbol{v}^{\mathsf{L}} = \overline{\boldsymbol{v}}^{\mathsf{L}} + \widetilde{\boldsymbol{v}}^{\mathsf{L}}$, where $\overline{\boldsymbol{v}}^{\mathsf{L}} = \langle \boldsymbol{v}^{\mathsf{L}} \rangle$.

We define some important statistical quantities of interest. The Eulerian velocity correlation function is defined by

$$R_{\boldsymbol{v}}(\boldsymbol{x}_1,\boldsymbol{x}_2,t_1,t_2) = \langle \widetilde{\boldsymbol{v}}(\boldsymbol{x}_1,t_1)\widetilde{\boldsymbol{v}}(\boldsymbol{x}_2,t_2)^* \rangle, \tag{5}$$

which is an outer product of the velocity fluctuations. The Lagrangian velocity correlation function of particle drifter pairs is given by

$$\begin{aligned} R^{\mathsf{L}^2}_{\boldsymbol{v}}(\boldsymbol{x}_1,\boldsymbol{x}_2,t_1,t_2) &= \langle \widetilde{\boldsymbol{v}}^{\mathsf{L}}(\boldsymbol{x}_1,t_1)\widetilde{\boldsymbol{v}}^{\mathsf{L}}(\boldsymbol{x}_2,t_2)^* \rangle \\ &= \langle \widetilde{\boldsymbol{v}}(\boldsymbol{X}(\boldsymbol{x}_1,t_1),t_1)\widetilde{\boldsymbol{v}}(\boldsymbol{X}(\boldsymbol{x}_2,t_2),t_2)^* \rangle, \end{aligned} \tag{6}$$

and the Lagrangian autocorrelation function of a single drifter is given by

$$R^{\mathsf{L}}_{\boldsymbol{v}}(\boldsymbol{\alpha},t_1,t_2) = R^{\mathsf{L}^2}_{\boldsymbol{v}}(\boldsymbol{\alpha},\boldsymbol{\alpha},t_1,t_2) = \langle \widetilde{\boldsymbol{v}}^{\mathsf{L}}(\boldsymbol{\alpha},t_1)\widetilde{\boldsymbol{v}}^{\mathsf{L}}(\boldsymbol{\alpha},t_2)^* \rangle. \tag{7}$$

Knowledge of the Lagrangian velocity correlation function $R^{\mathsf{L}^2}_{\boldsymbol{v}}$ fully describes the statistical correlations between positions of particle pairs moving throughout the flow. The Lagrangian autocorrelation function $R^{\mathsf{L}}_{\boldsymbol{v}}$ fully describes the second order moment of a single particle in time. In general, Eulerian and Lagrangian statistics are not equivalent since $\boldsymbol{v}$ and $\boldsymbol{v}^{\mathsf{L}}$ are not equal for most nontrivial flow fields.

When the statistics of the velocity field are homogeneous and stationary, the correlations depend only on the separation of spatial positions and time. This means that the correlation function is invariant under spatial and temporal translations,

$$R_{\boldsymbol{v}}(\boldsymbol{x}_1,\boldsymbol{x}_1+\boldsymbol{x},t_1,t_1+t) = R_{\boldsymbol{v}}(\boldsymbol{x},t). \tag{8}$$

Similarly, the autocorrelation functions would then only depend on relative time. For random fields that are homogeneous and stationary, the mean must be constant, and thus, at a minimum, the structure of the velocity field is contained in the correlation function.

The mean tracer displacement and the tracer's fluctuations about the mean are given by, respectively,

$$\begin{aligned} \overline{\boldsymbol{X}}(\boldsymbol{\alpha},t) &= \langle \boldsymbol{X} \rangle = \boldsymbol{\alpha} + \int_0^t \overline{\boldsymbol{v}}^{\mathsf{L}}(\boldsymbol{\alpha},s)\,ds, \\ \widetilde{\boldsymbol{X}}(\boldsymbol{\alpha},t) &= \boldsymbol{X} - \langle \boldsymbol{X} \rangle = \int_0^t \widetilde{\boldsymbol{v}}^{\mathsf{L}}(\boldsymbol{\alpha},s)\,ds. \end{aligned} \tag{9}$$

The tracer's mean-square displacement (i.e., the variance or tracer dispersion) can then be shown to be given by

$$\begin{aligned} \sigma^2_{\boldsymbol{X}}(t) &= \langle \widetilde{\boldsymbol{X}}(\boldsymbol{\alpha},t)\widetilde{\boldsymbol{X}}(\boldsymbol{\alpha},t)^* \rangle = \int_0^t \int_0^t R^{\mathsf{L}}(\boldsymbol{\alpha},s,s')\,ds\,ds' \\ &= 2\int_0^t (t-\tau)R^{\mathsf{L}}(\tau)\,d\tau, \end{aligned} \tag{10}$$

where the last equality holds if the velocity field is homogeneous and stationary, which can be shown using a change of variables. We can, in principle, characterize both short-term and long-term dispersion behaviors from Eq. (10). Standard derivations show that at short-times the dispersion grows at a ballistic rate, $\sigma^2_{\boldsymbol{X}}(t) \sim t^2$ and at long times the growth is diffusive, i.e., ordinary diffusion $\sigma^2_{\boldsymbol{X}}(t) \sim t$, if the integral $\int_0^\infty R^{\mathsf{L}}$ is finite and nonzero.

III. A GENERAL RANDOM TURBULENT VELOCITY MODEL WITH A RANDOM SPATIAL MEAN

We consider a two-dimensional, incompressible random velocity model on a periodic domain given by

$$\boldsymbol{v}(\boldsymbol{x},t) = \boldsymbol{w}(t) + \boldsymbol{u}(\boldsymbol{x},t) = \boldsymbol{w}(t) + \sum_{1\le|k|\le\Lambda} a_{\boldsymbol{k}}(t)\frac{i\boldsymbol{k}^{\perp}}{k}e^{i\boldsymbol{k}\cdot\boldsymbol{x}}, \quad a^*_{-\boldsymbol{k}} = a_{\boldsymbol{k}}, \tag{11}$$

on a total grid of $N = (2\Lambda+1)^2$ points, consisting of a spatially uniform mean $\boldsymbol{w}$ and fluctuations $\boldsymbol{u}$. The model in Eq. (11) represents the common situation where a fluid is moving under some mean flow effects due to external forces or geometric influences plus local effects due to turbulent fluctuations. The wavevector is denoted by $\boldsymbol{k}$ and $\boldsymbol{k}^{\perp}$ represents a counterclockwise rotation by 90° and the factor $i\boldsymbol{k}^{\perp}/k$ enforces the incompressibility constraint.

The dynamics of the background mean $\boldsymbol{w}$ and the Fourier coefficients $a_{\boldsymbol{k}}$, representing fluctuations relative to the background mean, are given by, respectively,

$$d\boldsymbol{w}(t) = \left((-\Gamma_0 + \Omega_0)\boldsymbol{w}(t) + \boldsymbol{f}_0\right)dt + \Sigma_0\,d\boldsymbol{W}_0(t), \tag{12}$$

$$da_{\boldsymbol{k}}(t) = \left((-d_{\boldsymbol{k}} + i\omega_{\boldsymbol{k}})a_{\boldsymbol{k}}(t) + f_{\boldsymbol{k}}\right)dt + \sigma_{\boldsymbol{k}}\,dW_{\boldsymbol{k}}(t), \tag{13}$$

where Ω_0 is a skew-symmetric constant matrix representing rotation effects, Γ_0 is a symmetric positive-definite constant matrix representing dissipation, and Σ_0 is a constant positive definite diagonal diffusion matrix. Each Fourier mode is an Ornstein-Uhlenbeck process with constant damping $d_{\boldsymbol{k}}$, dispersion $\omega_{\boldsymbol{k}}$, and diffusion $\sigma_{\boldsymbol{k}}$. The forcing terms $\boldsymbol{f}_0$ and $f_{\boldsymbol{k}}$ are assumed constant. The noise $W_{\boldsymbol{k}}$ is a circularly symmetric complex standard Wiener process and $\boldsymbol{W}_0$ is a real valued standard Wiener process.

The background mean $\boldsymbol{w}$ is a spatially uniform sweeping flow, which is a superposition of a constant mean sweep and a randomly fluctuating sweep, modeling large-scale motions across structures represented by $\boldsymbol{u}$ that models coherent shears and jets. The complex valued Fourier coefficients, $a_{\boldsymbol{k}}$, represent time varying random velocity gradients. The proposed velocity model is exactly solvable with explicit statistics. The time varying coefficients for the mean and fluctuations both satisfy constant coefficient stochastic differential equations (12) and (13), respectively, which can be solved through an integrating factor. The solution of the background mean is provided in Appendix B 1 and the Fourier coefficients in Appendix B 2. We remark that more general forcing of the form $f = Ae^{i\omega_0(k)t}$ could also be considered in the model, but this considerably complicates the resulting analysis so we refrain from the generalization.

The tracer particle paths are governed by the advection-diffusion equation in Eq. (1). Exact solutions satisfy the following (random) characteristics of this partial differential equation, which shows that the tracer particles are advected by the fluid velocity plus forcing due to molecular diffusion:

$$d\boldsymbol{X}(t) = \boldsymbol{v}(\boldsymbol{X}(t), t)\, dt + \Sigma_X\, d\boldsymbol{W}_X(t) \tag{14}$$

$$= \left(\boldsymbol{w}(t) + \sum_{\boldsymbol{k}\in I_N} a_{\boldsymbol{k}}(t) \frac{i\boldsymbol{k}^\perp}{k} e^{i\boldsymbol{k}\cdot\boldsymbol{X}(t)} \right) dt + \Sigma_X\, d\boldsymbol{W}_X(t), \tag{15}$$

where $\boldsymbol{W}_X$ is a real valued standard Wiener process and Σ_X is a diagonal noise matrix with (σ_x, σ_y) diagonal entries (we assume, in general, that $\sigma_x \neq \sigma_y$, corresponding to anisotropic diffusivity). The noise can be interpreted either as molecular diffusivity ($\sigma_i = \sqrt{2\kappa_i}$) or as an instrumental "observational" error in the context of data assimilation for drifters under pure advection (this involves recovery the flow field by "filtering" away the noise represented by this term).

IV. THE RANDOM TURBULENT SHEAR TEST MODEL FOR LAGRANGIAN PARTICLES

An important class of flows are those that are shear dominated, which are commonly encountered in various applications. We consider random shear flows under random cross-sweep processes [represented by the background mean term $\boldsymbol{w}(t)$] for the velocity model given in Eq. (12). The shear model we study is general and considers both deterministic and random cross-sweep processes that are superimposed on the random shear component.

The general form of a shear flow aligned along the horizontal axes is given by

$$\boldsymbol{v}(\boldsymbol{x}, t) = \boldsymbol{w}(t) + u(y, t)\mathbf{e}_x, \tag{16}$$

where $\mathbf{e}_x$ is a Cartesian unit vector along the x-axis. The structure of this velocity model involves a shear along the horizontal direction, with large scale sweeping motions from $\boldsymbol{w}$. The random cross-sweep process (acting perpendicular to the shearing direction) is represented by $w_y(t)$, where $\boldsymbol{w}(t) = (w_x(t), w_y(t))$.

Considering the velocity model in Eq. (11), shear flows of the form in Eq. (16) occur when the Fourier modes are all aligned parallel to the horizontal axes. For such velocity models, the random shear component thus has the form

$$u(y, t) = \sum_{1\le|k|\le\Lambda} a_k(t) \frac{-ik}{|k|} e^{iky}, \quad a_k = a^*_{-k}, \tag{17}$$

since $\boldsymbol{k} = k\mathbf{e}_y$ and $\boldsymbol{k}^\perp = -k\mathbf{e}_x$. The Lagrangian trajectories $\boldsymbol{X}(t) = (X(t), Y(t))$ driven by such a flow are the solution of

$$dX(t) = \big(w_x(t) + u(Y(t), t)\big)\, dt + \sigma_x\, dW_x(t), \tag{18}$$

$$dY(t) = w_y(t)\, dt + \sigma_y\, dW_y(t). \tag{19}$$

We study the Lagrangian and Eulerian statistics for this exact shear flow model and explore how the sweeping and shearing components of the flow interact in determining tracer transport.

We will show that the Lagrangian correlation function due to the shear leads to additional phase shifts from the cross-sweep process mean and shorter correlations due to both fluctuations of the cross-sweep process and molecular diffusion of the vertical tracer path, when compared to the Eulerian correlation function.

A. Overview on the structure of the Lagrangian statistics for more general shear models

Before deriving explicit results on the specific shear model in Eq. (17), we first provide an overview on the structure of the Lagrangian statistics that apply to general shear models. The derivation here will be succinct since detailed derivations are provided later with reference to the exact shear model in Eq. (17). Our aim here is to demonstrate the general features that are independent of the exact nature of the shear flow with minimal assumptions on its structure.

Assume the velocity field is stationary and homogeneous. First, note that the vertical tracer particle motion is given by

$$Y(\boldsymbol{\alpha}, t) = \alpha_y + \int_0^t w_y(s)\, ds + \sigma_y W_y(t), \tag{20}$$

where $\boldsymbol{\alpha} = (\alpha_x, \alpha_y)$, which we denote more simply by $Y(\alpha_y, t)$. The Lagrangian correlation function for the shear term between points α_{y1} and α_{y2} and times t and t' is then

$$R_u^{\mathrm{L}_2}(\alpha_y, \alpha_y + y, t, t') = \langle u(Y(\alpha_{y1}, t), t) u(Y(\alpha_{y2}, t'), t') \rangle \tag{21}$$

$$= \left\langle u\left(\alpha_{y1} + \int_0^t w_y(s)\, ds + \sigma_y W_y(t), t\right) \times u\left(\alpha_{y2} + \int_0^{t'} w_y(s)\, ds + \sigma_y W_y(t'), t'\right) \right\rangle. \tag{22}$$

To evaluate this expression and relate it to the Eulerian correlation function, we can freeze randomness that appears due to the cross-sweep and Wiener process terms, take an average over randomness due to shear v, and then take another average to account for randomness due to the frozen random terms, by application of the total law of expectations. This procedure gives

$$R_u^{\mathrm{L}_2}(y, t) = \left\langle R_u\left(y + \int_t^{t+\tau} w_y(s)\, ds + \sigma_y \int_t^{t+\tau} dW_y(s), \tau\right) \right\rangle, \tag{23}$$

where we have used stationarity and homogeneity of the correlation function and have defined $y = \alpha_{y2} - \alpha_{y1}$ and $\tau = t' - t$. This expression shows that the Lagrangian correlation function is an average of the Eulerian correlation function evaluated over ensembles of the cross-sweep process and diffusion. We see that flows without a cross-sweep and no diffusion, the Eulerian and Lagrangian correlation functions are equivalent.

We can also relate the Lagrangian correlation function to the Eulerian energy spectra $E(k, \omega)$using the Fourier transform relations of the correlation and energy spectrum,

$$R_u(y,\tau) = \iint e^{iky+i\omega\tau} E(k,\omega)\, dk\, d\omega. \tag{24}$$

Note that the expressions appearing in between parentheses in Eq. (23) can be effectively replaced by $Y(y, \tau)$ since it is only the relative time difference τ that is important. Substituting Eq. (23) into the above relation, we find

$$R_u^{\mathrm{L}^2}(y,\tau) = \iint e^{i\omega\tau} e^{iky} \left\langle e^{ik\int_t^{t+\tau} w_y(s)\, ds + ik\sigma_y \int_t^{t+\tau} dW_y(s)} \right\rangle \times E(k,\omega)\, dk\, d\omega. \tag{25}$$

If the mean $w_y(t)$ is also Gaussian, this expression can be further simplified using the property $\langle e^{itY}\rangle = e^{i\langle Y\rangle t - \frac{1}{2}\mathrm{Var}(Y)t^2}$ for a Gaussian variable Y. The following simplified expression is then obtained, relating the Lagrangian correlation function to the kinetic energy spectrum of the shear component:

$$R_u^{\mathrm{L}^2}(y,t) = \iint e^{i\omega t} e^{ik(y+\overline{w}_y\tau)} e^{-\frac{1}{2}k^2\sigma_y^2\tau} e^{-k^2\int_0^\tau (\tau-s)R_{w_y}(s)\, ds} \times E(k,\omega)\, dk\, d\omega. \tag{26}$$

This clearly demonstrates oscillations due to the deterministic mean of the cross-sweep and shorter correlations due to both fluctuations from the cross-sweep and particle diffusivity.

V. EXPLICIT EULERIAN VELOCITY AND CORRELATION FUNCTION

As mentioned, the exact solution of the general velocity field, which applies to the aligned shear model in Sec. IV, is provided in Appendix B. The Eulerian correlation function is the sum of the correlation function of the background mean $\boldsymbol{w}(t)$, derived in Eq. (B9), and the correlation function for the shear term $u(y, t)$. Using the exact solution of each Fourier mode in Appendix B 2, it is possible to show by the same technique used to derive the temporal correlation function of each Fourier mode that the *Eulerian correlation function* for the shear $u(y, t)$ in the equilibrium regime is homogeneous in space and stationary in time and is explicitly given by

$$R_u(y,\tau) = \sum_{1\le|k|\le\Lambda} \frac{\sigma_k^2}{2d_k} e^{(-d_k - i\omega_k)\tau} e^{-iky}. \tag{27}$$

VI. DERIVATION OF THE LAGRANGIAN VELOCITY AND CORRELATION FUNCTION

Next, we first discuss the structure of the Lagrangian velocity for the shear model. We show that the aligned shear model permits explicit formulas for the mean Lagrangian velocity and velocity fluctuations, which depend on the statistics of vertical tracer paths. We use these results to derive the Lagrangian velocity correlation function in Sec. VI E.

A. General structure of the Lagrangian velocity

Recall the definition of the Lagrangian velocity field in terms of the Eulerian velocity,

$$\boldsymbol{v}^{\mathrm{L}}(\boldsymbol{\alpha},t) = \boldsymbol{v}(\boldsymbol{X}(\boldsymbol{\alpha},t),t) = \boldsymbol{w}(t) + u(Y(\boldsymbol{\alpha},t),t)\mathbf{e}_x. \tag{28}$$

For the special aligned shear flow, only the vertical component of the Lagrangian tracer trajectory enters the horizontal component of the velocity field since the vertical component is unaffected by the shear. The Eulerian and Lagrangian velocities thus coincide in the vertical direction and we can directly integrate the equations to determine the vertical particle trajectory, from Eq. (19),

$$Y(\boldsymbol{\alpha},t) = \alpha_y + \int_0^t w_y(s)\, ds + \sigma_y W_y(t), \tag{29}$$

and substitute the solution into the Eulerian shear velocity. We thus obtain that the *Lagrangian velocity* is explicitly

$$v_x^{\mathrm{L}}(\boldsymbol{\alpha},t) = w_x(t) + \sum_{1\le|k|\le\Lambda} a_k(t)\frac{-ik}{|k|} e^{ikY(\boldsymbol{\alpha},t)}, \tag{30}$$

$$v_y^{\mathrm{L}}(\boldsymbol{\alpha},t) = w_y(t). \tag{31}$$

We first study the statistics of the mean vertical path in Sec. VI B since the shear statistics depends on it. Afterward, we utilize these results to derive the Lagrangian mean velocity. From the Lagrangian mean velocity, we can then compute the Lagrangian velocity fluctuations and thus the Lagrangian velocity correlation function.

B. Statistics of vertical tracer trajectories

Consider the vertical tracer trajectory. The mean of the vertical tracer path can be easily computed from

$$\overline{Y}(\boldsymbol{\alpha},t) = \langle Y\rangle = \alpha_y + \int_0^t \langle w_y(s)\rangle\, ds, \tag{32}$$

where $\langle w_y(s)\rangle$ is the imaginary part of the complex-valued representation of the background mean in Eq. (B6). Assuming the velocity field is in the statistically stationary regime, where $\overline{w} = -f_0/p_0$, we then find that the vertical tracer mean is

$$\overline{Y}(\boldsymbol{\alpha},t) = \alpha_y + \overline{w}_y t, \quad \text{where } \overline{w}_y = \mathrm{Im}\{-f_0/p_0\} = \frac{d_0 f_{0y} + \omega_0 f_{0x}}{d_0^2+\omega_0^2}, \tag{33}$$

which grows linearly in time $\overline{Y} \sim t$. To compute the variance $\sigma_Y^2(t)$, we first compute the equations for the deviations from its mean

$$\widetilde{Y}(\boldsymbol{\alpha},t) = Y - \langle Y\rangle = \int_0^t \widetilde{w}_y(s)\, ds + \sigma_y \int_0^t dW_y(s), \tag{34}$$

where $\widetilde{w}_y(t) = \mathrm{Im}\{w(t) - \langle w(t)\rangle\}$. Next,

$$\sigma_Y^2(t) = \langle \widetilde{Y}^2\rangle = \sigma_w^2(t) + \sigma_y^2 t = 2\int_0^t (t-\tau)R_{w_y}(\tau)\, d\tau + \sigma_y^2 t, \tag{35}$$

and since the diffusion matrix Σ_0 has diagonal entries that are equivalent and equal to σ_0 and the noise is circularly symmetric, the correlation of $w_y(t)$ is equal to half the real part of the correlation of the

complex process $w(t)$ in Eq. (B9). Explicit integration shows

$$\sigma_w^2(t) = 2\int_0^t (t-\tau)R_{w_y}(\tau)\,d\tau$$
$$= \frac{\sigma_0^2}{d_0(d_0^2+\omega_0^2)^2}\Big(\big(-d_0^2+\omega_0^2\big)+e^{-d_0 t}\big((d_0^2-\omega_0^2)\cos(\omega_0 t)$$
$$-2d_0\omega_0\sin(\omega_0 t)\big)\Big)+\left(\frac{\sigma_0^2}{(d_0^2+\omega_0^2)}\right)t. \tag{36}$$

For the case with zero rotation in the background mean $\omega_0 = 0$, the tracer dispersion simplifies to

$$\sigma_Y^2(t) = \left(\frac{\sigma_0^2}{d_0^2}+\sigma_y^2\right)t+\frac{\sigma_0^2}{d_0^3}(e^{-d_0 t}-1). \tag{37}$$

The long and short time behavior for the case with nonzero rotation is given by

$$\begin{aligned}\sigma_Y^2 &\sim \sigma_y^2 t+\frac{\sigma_0^2}{2d_0}t^2 \quad \text{for small } t,\\ \sigma_Y^2 &\sim \left(\frac{\sigma_0^2}{(d_0^2+\omega_0^2)}+\sigma_y^2\right)t \quad \text{for large } t.\end{aligned} \tag{38}$$

At long times, we have linear or diffusive growth of the tracer variance. We find that rotation reduces the diffusion rate at long times $t \gg d_0$, but does not manifest at short times. We also note that when the diffusion term is zero $\sigma_y = 0$, the tracer grows at a ballistic rate at short times $t \ll 1/d_0$, but when the molecular diffusion is nonzero, the variance grows linearly, as expected.

C. Equations for the mean Lagrangian velocity

Consider now the mean Lagrangian velocity. Taking the ensemble mean of the Lagrangian velocity leads to the Lagrangian mean velocity,

$$\overline{v}_x^{\mathsf{L}}(\boldsymbol{\alpha},t) = \overline{w}_x+\sum_{1\le|k|\le\Lambda}\frac{-ik}{|k|}\left\langle a_k(t)e^{ikY(\boldsymbol{\alpha},t)}\right\rangle, \tag{39}$$

$$\overline{v}_y^{\mathsf{L}}(\boldsymbol{\alpha},t) = \overline{w}_y. \tag{40}$$

We now simplify the ensemble average that appears above. Recall that the characteristic function of a random variable Y is defined as $\phi_Y(t) = \langle e^{itY}\rangle$. Explicit computation for a Gaussian random variable shows

$$\phi_Y(t) = e^{i\langle Y\rangle t-\frac{1}{2}\mathrm{Var}(Y)t^2}. \tag{41}$$

Since the drifter trajectory in the vertical direction Y is Gaussian, and since a_k is independent of Y,

$$\left\langle a_k(t)e^{ikY(\boldsymbol{\alpha},t)}\right\rangle = \langle a_k(t)\rangle e^{ik\langle Y(\boldsymbol{\alpha},t)\rangle-\frac{1}{2}k^2\mathrm{Var}(Y(\boldsymbol{\alpha},t))}$$
$$= \overline{a_k}e^{ik\overline{Y}(\boldsymbol{\alpha},t)-\frac{1}{2}k^2\sigma_Y^2(t)}, \tag{42}$$

where $\sigma_Y^2(t) = \mathrm{Var}(Y(\boldsymbol{\alpha},t))$. Substituting the equations for the mean of the shear mode and the vertical particle mean and variance from Sec. VI B, we find that the *mean Lagrangian velocity* is explicitly

$$\overline{v}_x^{\mathsf{L}}(\boldsymbol{\alpha},t) = \overline{w}_x+\sum_{1\le|k|\le\Lambda}\frac{ik}{|k|}\frac{f_k}{p_k}e^{ik(\alpha_y+\overline{w}_y t)-\frac{1}{2}k^2\sigma_Y^2(t)}, \tag{43}$$

$$\overline{v}_y^{\mathsf{L}}(\boldsymbol{\alpha},t) = \overline{w}_y. \tag{44}$$

D. Equations for the Lagrangian velocity fluctuations

Computing $\widetilde{\boldsymbol{v}}^{\mathsf{L}} = \boldsymbol{v}^{\mathsf{L}}-\overline{\boldsymbol{v}}^{\mathsf{L}}$, using the results from the Lagrangian mean calculations, we find that the Lagrangian velocity fluctuations are governed by

$$\widetilde{v}_x^{\mathsf{L}}(\boldsymbol{\alpha},t) = \widetilde{w}_x(t)+\sum_{1\le|k|\le\Lambda}e^{ik\langle Y(\boldsymbol{\alpha},t)\rangle}\frac{-ik}{|k|}$$
$$\times\left(a_k(t)e^{ik\widetilde{Y}(\boldsymbol{\alpha},t)}-\overline{a_k}e^{-\frac{1}{2}k^2\mathrm{Var}(Y(\boldsymbol{\alpha},t))}\right), \tag{45}$$

$$\widetilde{v}_y^{\mathsf{L}}(\boldsymbol{\alpha},t) = \widetilde{w}_y(t). \tag{46}$$

E. The Lagrangian correlation function along the shearing direction

Next, we consider the Lagrangian correlation function R^{L_2}. To proceed, note we have already derived the correlation function of the background velocity $\boldsymbol{w}$ and what remains is to determine the Lagrangian correlation of the shear term $u(y,t)$.

Considering the structure of the Lagrangian velocity

$$\boldsymbol{v}^{\mathsf{L}}(\boldsymbol{\alpha},t) = \boldsymbol{w}(t)+u(Y(\boldsymbol{\alpha},t),t)\mathbf{e}_1, \tag{47}$$

the correlation of the Lagrangian velocity has the form

$$R_{\boldsymbol{v}}^{\mathsf{L}_2}(\boldsymbol{\alpha}_1,\boldsymbol{\alpha}_2,t,t') = R_{\boldsymbol{w}}(t,t')+R_u^{\mathsf{L}_2}(\boldsymbol{\alpha}_1,\boldsymbol{\alpha}_2,t,t')\mathbf{e}_1\mathbf{e}_1^*, \tag{48}$$

which is a sum of the contribution due to the mean [which is known, see Eq. (B9)] and the unknown term from the shear. The Lagrangian correlation $R_u^{\mathsf{L}_2}$ is explicitly given by

$$R_u^{\mathsf{L}_2}(\boldsymbol{\alpha}_1,\boldsymbol{\alpha}_2,t,t') = \left\langle\widetilde{u}\big(Y(\boldsymbol{\alpha}_1,t),t\big)\widetilde{u}\big(Y(\boldsymbol{\alpha}_2,t'),t'\big)^*\right\rangle \tag{49}$$
$$= \left\langle\widetilde{u}\left(\alpha_{y1}+\int_0^t w_y(s)\,ds+\sigma_y W_y(t),t\right)\right.$$
$$\left.\times\,\widetilde{u}\left(\alpha_{y2}+\int_0^{t'} w_y(s)\,ds+\sigma_y W_y(t'),t'\right)^*\right\rangle. \tag{50}$$

We can simplify the above expression using the formula for the Lagrangian fluctuations in Sec. VI D, explicitly, or by application of the total law of expectations, which we demonstrate here. According to the total law of expectations, we can first fix the random term w_y, take the expectation over the noise, and then take a second expectation over w_y to obtain $R_u^{\mathsf{L}_2}$. The first expectation relates the Lagrangian correlation function to the Eulerian correlation function given in Eq. (27),

$$R_u^{\mathsf{L}_2}(\boldsymbol{\alpha}_1,\boldsymbol{\alpha}_2,t,t') = \left\langle R_u\big(Y(\boldsymbol{\alpha}_1,t),Y(\boldsymbol{\alpha}_2,t'),t,t'\big)\right\rangle \tag{51}$$
$$= \left\langle\sum_{1\le|k|\le\Lambda}\frac{\sigma_k^2}{2d_k}e^{-d_k(t'-t)}e^{-i\omega_k(t'-t)}e^{-ik(Y(\boldsymbol{\alpha}_2,t')-Y(\boldsymbol{\alpha}_1,t))}\right\rangle \tag{52}$$
$$= \left\langle\sum_{1\le|k|\le\Lambda}\frac{\sigma_k^2}{2d_k}e^{-d_k(t'-t)}e^{-i\omega_k(t'-t)}e^{-ik(\alpha_{y2}-\alpha_{y1})}\right.$$
$$\left.\times\,e^{-ik\left(\int_t^{t'}w_y(s)\,ds+\int_t^{t'}\sigma_y\,dW_y\right)}\right\rangle. \tag{53}$$

Next, let $t' = t + \tau$ and since the trajectory $Y(\boldsymbol{\alpha}, t)$ only depends on the initial condition in the y coordinate, we denote the difference between $\boldsymbol{\alpha}_2$ and $\boldsymbol{\alpha}_1$ by $y = \alpha_{y2} - \alpha_{y1}$; thus,

$$R_u^{\mathrm{L}_2}(y, t, t+\tau) = \sum_{1\le|k|\le\Lambda} \frac{\sigma_k^2}{2d_k} e^{-d_k\tau} e^{-i\omega_k\tau} e^{-iky} \times \left\langle e^{-ik\left(\int_t^{t+\tau} w_y(s)\,ds + \int_t^{t+\tau} \sigma_y\,dW_y\right)} \right\rangle. \tag{54}$$

We can now apply the result for the characteristic function of a Gaussian random variable again and use the results for the mean and variance of the vertical tracer trajectory to simplify the ensemble mean that appears in the equation above. We obtain that the *Lagrangian correlation function* is

$$R_u^{\mathrm{L}_2}(y, \tau) = \sum_{1\le|k|\le\Lambda} \frac{\sigma_k^2}{2d_k} e^{-d_k\tau} e^{-i\omega_k\tau} e^{-iky} e^{-ik\overline{w}_y\tau} e^{-\frac{1}{2}k^2\sigma_Y^2(\tau)}, \tag{55}$$

where σ_Y^2 and $\overline{w}_y$ are given explicitly in Sec. VI B. The Lagrangian autocorrelation function is obtained by setting $y = 0$,

$$R_u^{\mathrm{L}}(\tau) = R_u^{\mathrm{L}_2}(0, \tau) = \sum_{1\le|k|\le\Lambda} \frac{\sigma_k^2}{2d_k} e^{-d_k\tau} e^{-i\omega_k\tau} e^{-ik\overline{w}_y\tau} e^{-\frac{1}{2}k^2\sigma_Y^2(\tau)}. \tag{56}$$

VII. COMPARISON OF THE LAGRANGIAN AND EULERIAN CORRELATION ALONG THE SHEAR

Before studying the dispersive properties of Lagrangian particles along the shear, we highlight and discuss the differences between the Eulerian and Lagrangian correlation functions.

Consider the shear velocity model in Eq. (17) with a single mode $\Lambda = 1$. Recall that the Eulerian correlation, from Eq. (27), at a fixed location in space, is given by

$$R_u(\tau) \equiv R_u(0, \tau) = \frac{\sigma_k^2}{d_k} e^{-d_k\tau} \cos(\omega_k\tau), \tag{57}$$

and the Lagrangian correlation, following a single particle in space, from Eq. (55) with $y = 0$, and assuming a deterministic mean $\sigma_Y^2(t) = \sigma_y^2 t$, is given by

$$R_u^{\mathrm{L}}(\tau) = R_u^{\mathrm{L}_2}(0, \tau) = \frac{\sigma_k^2}{d_k} e^{-(d_k + \frac{1}{2}k^2\sigma_y^2)\tau} \cos((\omega_k + k\overline{\omega}_y)\tau). \tag{58}$$

The absolute difference between the Eulerian and Lagrangian correlation functions for a nondispersive mode, for which $\omega_k = 0$, is given by

$$|R_u(\tau) - R_u^{\mathrm{L}}(\tau)| = R_u(\tau) \times \left(1 - e^{-\frac{1}{2}k^2\sigma_y^2\tau} \cos(k\overline{\omega}_y\tau)\right). \tag{59}$$

A comparison is shown in Fig. 1. Observe the effects of the background mean cross-sweep $\overline{w}_y$ magnitude on the Lagrangian velocity autocorrelation function, which results in faster decaying correlations that oscillate more rapidly compared to the Eulerian correlation function. The magnitude of the vertical mean impacts the oscillation rate, and the magnitude of the molecular diffusion σ_y affects how rapidly the correlations decay. Flows with a dominant vertical mean have rapidly oscillating Lagrangian correlations. In addition, flows with a highly energetic random mean and large molecular diffusivity have short correlations with rapid decay. For flows with a deterministic cross-sweep, the correlations are closest at every $2\pi/k\overline{w}_y$ period in a single mode system. These factors result in large differences between the Eulerian and Lagrangian correlation functions, and in summary:

- Flows with a strong vertical mean results in correlations with rapid oscillations.
- Flows with strongly energetic cross-sweeps and large molecular diffusivity have short range correlations that rapidly decay.

In Sec. VIII, we discuss the physical interpretation that causes the difference between the Lagrangian and Eulerian statistics, which stem from an interplay between the mean sweeps and the shear flow.

VIII. LAGRANGIAN STATISTICS AND MIXING BEHAVIOR ALONG THE SHEARING DIRECTION

Here, we derive equations that predict the mixing behavior (tracer particle dispersion) along the shearing direction $\sigma_X^2(t)$ in various limits and flow regimes. We study both the short time asymptotic dispersion rate as $t \to 0$ and the long time asymptotic dispersion rate for $t \to \infty$. We later link these predictions with numerical simulations, comparing regimes where various terms dominate, in Sec. IX, referring back to the discussion here.

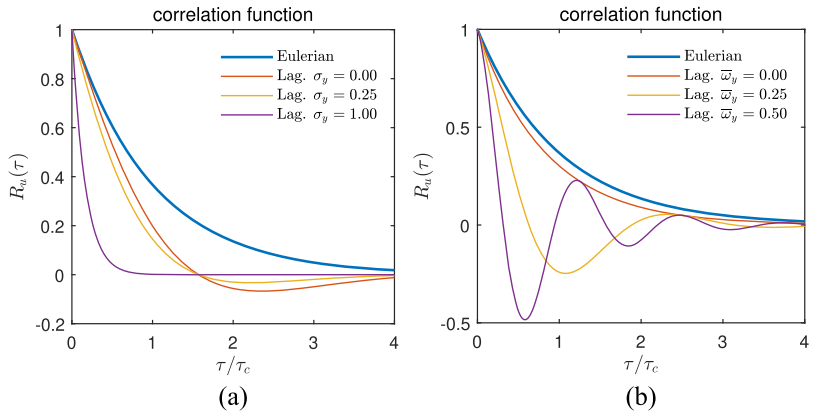

FIG. 1. Comparison of the Eulerian (solid blue) and Lagrangian correlation function as the model mean and molecular diffusion are varied. In (a), we demonstrate the effect on the correlation as the molecular diffusivity σ_y is varied. In (b), we demonstrate the effects on the correlation as the cross-sweep mean magnitude $\overline{w}_y$ is varied. Here, $\tau_c = 1/\nu$, where ν is the model viscosity (see Sec. IX). (a) Correlation function for fixed $\overline{w}_y = 0.1$ and varying molecular diffusivity σ_y. (b) Correlation function for fixed $\sigma_y = 0.2$ and varying cross-sweep mean magnitude $\overline{w}_y$.

We first discuss models with a purely deterministic mean, where an explicit formula can be derived for the tracer's mean-square displacement. This is developed for a single shear mode in Sec. VIII A and the general case in Sec. VIII B; we then discuss and interpret the results in Sec. VIII B 1. For shear flows with a general random background mean, we derive the dispersion characteristics in the short and long time limits in Sec. VIII C, where we also discuss the new physics that arises in this more general case.

A. A single shear mode with a constant background mean

The simplest setting involves a single shear mode and a deterministic sweep. In this setting, the vertical tracer variance is simply $\sigma_Y^2(t) = \sigma_y^2 t$ [Eq. (37) with $\sigma_0 = 0$] and the reduced equation for the autocorrelation function for the tracer along the shearing direction simplifies to

$$R_u^{\mathrm{L}}(\tau) = \frac{\sigma_k^2}{2d_k} 2\mathrm{Re}\{e^{-d_k\tau} e^{-i\omega_k\tau} e^{-ik\overline{w}_y\tau} e^{-\frac{1}{2}k^2\sigma_y^2\tau}\}. \tag{60}$$

We define an *effective damping and dispersion* by

$$\tilde{d}_k = d_k + \frac{1}{2}k^2\sigma_y^2 \quad \text{and} \quad \tilde{\omega}_k = \omega_k + k\overline{w}_y, \tag{61}$$

respectively, and then

$$R_u^{\mathrm{L}}(\tau) = \frac{\sigma_k^2}{d_k} \mathrm{Re}\{e^{(-\tilde{d}_k - i\tilde{\omega}_k)\tau}\}. \tag{62}$$

The Lagrangian particle variance for the shear term is obtained by integration,

$$\begin{aligned}\sigma_u^2(t) &= 2\int_0^t (t-\tau) R_u^{\mathrm{L}}(\tau)\, d\tau \\ &= \frac{2\sigma_k^2}{(\tilde{d}_k^2 + \tilde{\omega}_k^2)} t + \frac{2\sigma_k^2}{d_k(\tilde{d}_k^2 + \tilde{\omega}_k^2)^2}\Big((-\tilde{d}_k^2 + \tilde{\omega}_k^2) \\ &\quad + e^{-\tilde{d}_k t}\big((\tilde{d}_k^2 - \tilde{\omega}_k^2)\cos(\tilde{\omega}_k t) - 2\tilde{d}_k\tilde{\omega}_k \sin(\tilde{\omega}_k t)\big)\Big).\end{aligned} \tag{63}$$

The last contribution to the variance involves diffusion from the Brownian noise term,

$$\sigma_X^2(t) = \sigma_u^2(t) + \sigma_x^2 t, \tag{64}$$

and thus, the total behavior of the tracer dispersion along the shear is governed by

$$\sigma_u^2 \sim \sigma_x^2 t + \frac{\sigma_k^2}{d_k} t^2 \ \text{ for small } t \ \text{ and } \ \sigma_u^2 \sim \left(\frac{2\sigma_k^2}{\tilde{d}_k^2 + \tilde{\omega}_k^2} + \sigma_x^2\right) t \ \text{ for large } t. \tag{65}$$

B. General shear flows with a constant background mean

For multiple shear modes, the result is identical to the single shear mode case, except the contribution due to all the various modes is summed. The total variance from the shearing flow is therefore

$$\begin{aligned}\sigma_u^2(t) = \sum_{1\le k\le\Lambda} \frac{2\sigma_k^2}{d_k(\tilde{d}_k^2 + \tilde{\omega}_k^2)^2}\Big((-\tilde{d}_k^2 + \tilde{\omega}_k^2) + d_k(\tilde{d}_k^2 + \tilde{\omega}_k^2)t \\ + e^{-\tilde{d}_k t}((\tilde{d}_k^2 - \tilde{\omega}_k^2)\cos(\tilde{\omega}_k t) - 2\tilde{d}_k\tilde{\omega}_k \sin(\tilde{\omega}_k t))\Big),\end{aligned} \tag{66}$$

where the total variance of X trajectories is again given by $\sigma_X^2(t) = \sigma_u^2(t) + \sigma_x^2 t$. The tracer variance has the following short and long time behavior:

$$\begin{aligned}\sigma_X^2 &\sim \sigma_x^2 t + \sum_{1\le k\le\Lambda} \frac{\sigma_k^2}{d_k} t^2 \quad \text{for small } t, \\ \sigma_X^2 &\sim \left(\sum_{1\le k\le\Lambda} \frac{2\sigma_k^2}{\tilde{d}_k^2 + \tilde{\omega}_k^2} + \sigma_x^2\right) t \quad \text{for large } t.\end{aligned} \tag{67}$$

1. Mixing behavior in various limits

We make the following observations regarding the tracer variance behavior:

- At small times, if the tracer particles are driven by molecular diffusion σ_x, diffusion dominates over the ballistic growth rate due to the shear. When there is zero molecular diffusion $\sigma_x = 0$, the tracer variance grows at a ballistic rate.
- Assuming zero molecular diffusion and a shear with a power law spectrum $E_k = \mathcal{E}|k|^{-\alpha}$, we then find that the short time behavior is given by

$$\sigma_X^2 \sim \left(2\mathcal{E}\sum_{1\le k\le\Lambda} |k|^{-\alpha}\right) t^2, \tag{68}$$

  and hence, the diffusion is determined entirely by the spectral slope from the shearing component when $\sigma_x = 0$.
- At long times, the behavior of the tracer along the shearing direction is diffusive. To understand the effects of each term, consider the effective damping and dispersion,

$$\tilde{d}_k = d_k + \frac{1}{2}\sigma_y^2 k^2 \quad \text{and} \quad \tilde{\omega}_k = \omega_k + k\overline{w}_y. \tag{69}$$

  For simplicity, considering a scenario with nondispersive modes $\omega_k = 0$ and viscous damping $d_k = \mu k^2$, we then find that the dispersion due to the shear is

$$\sigma_X^2 \sim \left(\sum_{1\le k\le\Lambda} \frac{4\mu\mathcal{E}|k|^{-\alpha}}{(\mu + \frac{1}{2}\sigma_y^2)^2 k^2 + \overline{\omega}_y^2} + \sigma_x^2\right) t. \tag{70}$$

  Observe that the cross sweeps lead to reduced dispersion rates, which we expect since the cross-sweeps push particles across streamlines and thus impede them from dispersing along the shearing direction. We also see how molecular diffusion along the vertical direction enhances viscosity through a similar mechanism as described for the cross-sweeps, but which is scale dependent.

For large wavenumbers, the effective contribution to the dispersion is minimal since

$$\frac{4\mu\mathcal{E}|k|^{-\alpha}}{(\mu + \frac{1}{2}\sigma_y^2)^2 k^2 + \overline{\omega}_y^2} \sim \frac{4\mu\mathcal{E}}{(\mu + \frac{1}{2}\sigma_y^2)^2}|k|^{-\alpha-2}, \quad \text{for large } k. \tag{71}$$

Consider the scenario where the viscosity is large relative to the cross sweep magnitude and molecular diffusivity, we then find that shear variance is given by

$$\sigma_u^2 \sim \left(\sum_{1\le k\le \Lambda} \frac{4\mathcal{E}}{\mu} |k|^{-\alpha-2} \right) t, \quad \text{for large } \mu, \tag{72}$$

which is a regime where the tracer's vertical motion $Y(t)$ has minimal contribution to the Lagrangian velocity.

- An elementary observation is that the effective reduction on the dispersion rate due to cross-sweeps is mitigated if the shear is dispersive, i.e., $\omega_k \neq 0$. In the extreme scenario, it can be suppressed by a shear flow with advection with speed $c = \overline{w}_y$ and $\omega_k = -ck$. When the cross-sweeps are zero, the particle dispersion rate is only reduced due to contributions from molecular diffusivity σ_y in the vertical direction.

C. Shear flows with a general random background mean: Short and long time behavior

Now, consider the most general case involving random cross-sweeps with a deterministic mean. First consider a single shear mode for which the Lagrangian autocorrelation is given by

$$R_u^{\mathrm{L}}(\tau) = \frac{\sigma_k^2}{2d_k} 2\mathrm{Re}\{ e^{-d_k\tau} e^{-i\omega_k\tau} e^{-ik\overline{w}_y\tau} e^{-\frac{1}{2}k^2\sigma_Y^2(\tau)} \}, \tag{73}$$

where the variance of the vertical tracer dispersion has already been computed to be

$$\sigma_Y^2(t) = \sigma_w^2(t) + \sigma_y^2 t, \tag{74}$$

where σ_w^2 is given in Eq. (36). Integrating, the resulting autocorrelation function is unwieldy for the full particle dispersion along the shear σ_u^2 (it involves exponentials of exponential and trigonometric functions). We instead study the behavior of the tracer's mean-square displacement at short and long times. To proceed, recall the behavior of the vertical tracer variance in these limits, from Eq. (38),

$$\begin{aligned} \sigma_Y^2 &\sim \sigma_y^2 t + \frac{\sigma_0^2}{2d_0} t^2 \quad \text{for small } t, \\ \sigma_Y^2 &\sim \left(\frac{\sigma_0^2}{(d_0^2+\omega_0^2)} + \sigma_y^2 \right) t \quad \text{for large } t. \end{aligned} \tag{75}$$

1. Short time behavior

At short times, the diffusion rate, for zero molecular diffusion, is again dominated by Brownian noise at a linear rate determined by σ_x. The effective damping and dispersion in the short time limit are given by

$$\tilde{d}_k = d_k + \frac{1}{2}\sigma_y^2 k^2 \quad \text{and} \quad \tilde{\omega}_k = \omega_k + \overline{w}_y k. \tag{76}$$

At these time scales, the effects of the random cross-sweeps do not manifest. The autocorrelation function of a single shear mode is thus

$$R_u^{\mathrm{L}}(\tau) = \frac{\sigma_k^2}{d_k} \mathrm{Re}\{ e^{(-\tilde{d}_k - i\tilde{\omega}_k)\tau} e^{-\frac{1}{2}\frac{\sigma_0^2}{2d_0}\tau^2} \}, \tag{77}$$

and an expansion at small times shows that the dispersion due to the shear is identical to the deterministic cross sweep scenario; hence, the variance at short times has the scaling

$$\sigma_X^2 \sim \sigma_x^2 t + \left(\frac{\sigma_0^2}{(d_0^2+\omega_0^2)} + 2\mathcal{E} \sum_{1\le k\le\Lambda} |k|^{-\alpha} \right) t^2 \quad \text{for small } t. \tag{78}$$

2. Long time behavior

In the large time limit, we find that the effective damping and dispersion are

$$\tilde{d}_k = d_k + \frac{1}{2}\sigma_y^2 k^2 + \frac{\sigma_0^2}{2(d_0^2+\omega_0^2)} k^2 \quad \text{and} \quad \tilde{\omega}_k = \omega_k + \overline{w}_y k. \tag{79}$$

The additional term above in the effective damping equation, due randomness in the mean, acts identical to viscous damping. For the total tracer variance, we must also include the additional contribution to the total tracer particle variance along the shear from the random mean term, which is represented by σ_w^2 and is equivalent to its contribution to the vertical tracer variance, given in Eq. (36),

$$\sigma_X^2(t) = \sigma_w^2(t) + \sigma_u^2(t) + \sigma_x^2 t. \tag{80}$$

For the shear term above, the result from Sec. VIII B applies, except using the appropriate effective damping and dispersion relations defined in Eq. (79). We thus find that the total variance scales like

$$\sigma_X^2 \sim \left(\frac{\sigma_0^2}{(d_0^2+\omega_0^2)} + \sum_{1\le k\le\Lambda} \frac{2\sigma_k^2}{\tilde{d}_k^2+\tilde{\omega}_k^2} + \sigma_x^2 \right) t \quad \text{for large } t. \tag{81}$$

The same observations and intuition holds here as for the case with deterministic cross-sweeps at long times (see Sec. VIII B 1), except we now have enhanced damping due to the random component of the mean appearing in the effective damping relation.

If we again consider a fluid model with viscous damping $d_k = \mu k^2$ and zero dispersion, we find that variance due to the shear at long times scales like

$$\sigma_u^2 \sim \left(\sum_{1\le k\le\Lambda} \frac{4\mu\mathcal{E}|k|^{-\alpha}}{(\mu + \frac{1}{2}\sigma_y^2 + \frac{\sigma_0^2}{2(d_0^2+\omega_0^2)})^2 k^2 + \overline{\omega}_y^2} \right) t. \tag{82}$$

Note the effect of the random component of the mean enter the shear dispersion rate at long times. We make the following important observation regarding the background mean and its interaction with the shear:

- Random background fluctuations reduce dispersive mixing along the shear direction. A highly energetic background impedes particles from dispersion along the shear; the random fluctuations inhibit tracer particles from advection by the shear.
- Large rotation ω_0 enhances dispersion along the shear. Physically, strong rotation forces particles to rotate counterclockwise pushing them across streamlines as they are randomly swept along by the shear, which counteracts the noise in the mean preventing the particles from dispersing; the combined effect of this interplay leads to enhanced dispersion.

- A random mean with small time correlations, i.e., large damping $d_0 \gg 0$, acts on particles on very short time scales, which minimizes the impact of the random mean term, thus enhancing the mixing rate. Conversely, a mean with long time correlations, i.e., small damping $d_0 \ll 0$, blocks the shear and reduces the dispersion rate.

IX. NUMERICAL SIMULATION OF MODEL REGIMES AND TRACER DISPERSION STATISTICS

Here, we include numerical simulation in different model regimes and compare tracer dispersion statistics with theoretical predictions. We study important physical features that arise when certain model parameters dominate and connect them with the discussion in Sec. VIII.

Consider the aligned shear model described in Sec. IV,

$$\boldsymbol{v}(\boldsymbol{x},t) = \boldsymbol{w}(t) + u(y,t)\mathbf{e}_x, \tag{83}$$

where the spatial mean is given by

$$dw = \big((-d_0 + i\omega_0)w + f_0\big)\,dt + \sqrt{2}\sigma_0\,dW_0 \tag{84}$$

and the shear by

$$u(y,t) = \sum_{1\le|k|\le\Lambda} a_k(t)\frac{-ik}{|k|}e^{iky}, \quad a_k = a^*_{-k}, \tag{85}$$

$$da_k = \big((-d_k + i\omega_k)a_k + f_k\big)\,dt + \sigma_k\,dW_k. \tag{86}$$

The time scale of the flow is defined by $\tau_c = 1/\mu$, and the damping model is given by $d_k = \mu k^2$. We assume that molecular diffusivity is equivalent in both directions, i.e., $\sigma_X = \sigma_x = \sigma_y$. The forcing is specified as $f_0 = f_{0x} + if_{0y}$, with $f_{0x} = 0$. We consider a model with maximum wavenumber $\Lambda = 10$ and a spectrum with $E_k = \mathcal{E}|k|^{-\alpha}$, where $\mathcal{E} = 1.0$. Examples are included where we vary the energy of the fluctuations of the background mean defined by $E_0 = \sigma_0^2/2d_0$. We define the long time tracer dispersion or mixing rate along the shear parallel direction by $\overline{D} = \sigma_X^2(t)/2t$ for $t \to \infty$, which is simply one-half the time derivative of the tracer particle's mean-square displacement.

A. Numerical simulations in various test regimes

In Figs. 2–12, for demonstration, 10 tracer trajectories are plotted over a simulation length of 40 τ_c units. Statistics are carried out over a simulation of length $t = 600\ \tau_c$ and 250 particle drifter ensembles are used. The simulation domain is a 2π periodic box; however, we "unwrap" the tracer trajectories over the periodic domain to demonstrate their spatial extent. In the tracer variance plots, in Figs. 2–12, the dashed red line corresponds to the prediction in Eq. (78) and the solid red line to the prediction in Eq. (81). Note the close agreement with the predicted dispersion rates and those obtained by Monte Carlo simulations.

1. Tracer particle diffusion magnitude

We compare cases in Figs. 2 and 3 for varying tracer diffusion values σ_X in regimes with a small constant mean sweep. Observe how

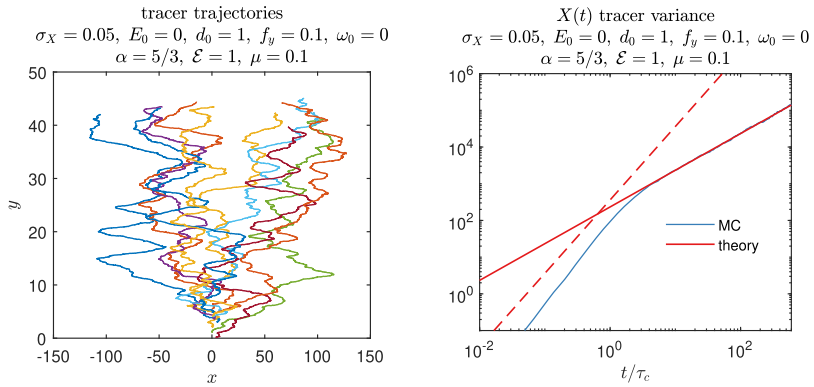

FIG. 2. Example where the tracer particle diffusivity is $\sigma_X = 0.05$. Tracer particle trajectories are plotted in the left pane and the tracer variance $\sigma_X^2(t)$ in the right pane.

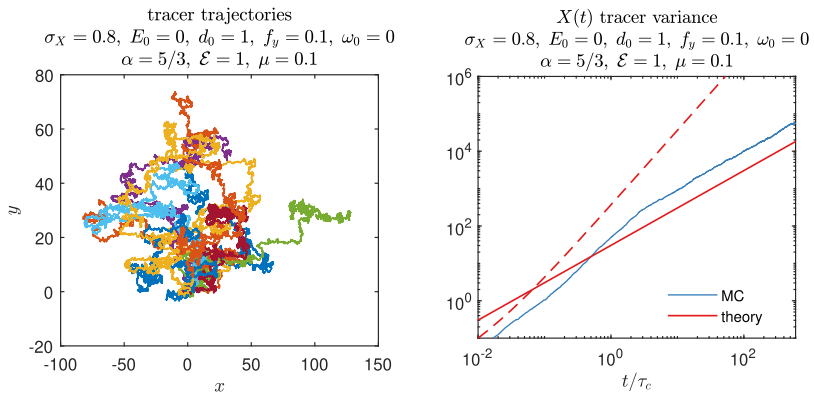

FIG. 3. Example where the tracer particle diffusivity is $\sigma_X = 0.8$. Tracer particle trajectories are plotted in the left pane and the tracer variance $\sigma_X^2(t)$ in the right pane.

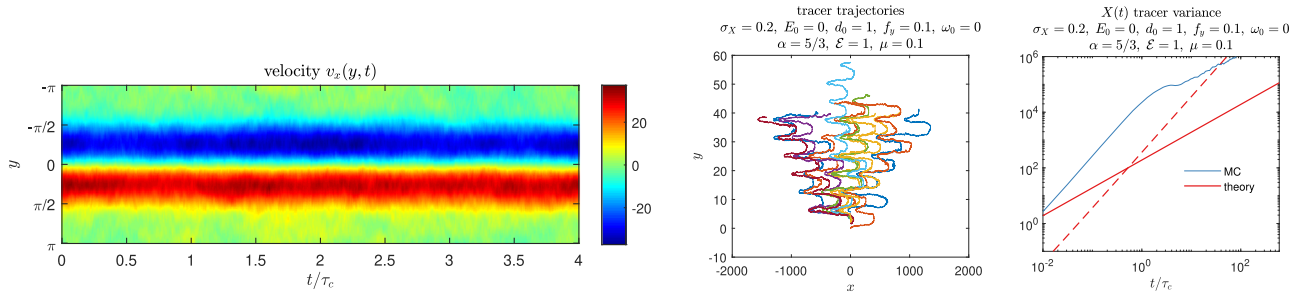

FIG. 4. Shear mode k has forcing specified by f_k; in this example, $f_1 = 1.0$, $f_2 = 2.0$, and $f_3 = 2.0$. Left pane plots the shear term $u(y, t)$, middle pane plots the tracer particle trajectories, and the right pane plots the tracer variance $\sigma_X^2(t)$.

larger values of the diffusion constant σ_X constrain the tracer trajectories from freely mixing and thus reduce the dispersion rate [see also Eq. (70)]. The long-time asymptotic mixing rate for the example with smaller molecular diffusion $\sigma_X = 0.05$ is $\overline{D} = 23.5$, whereas for the example with large diffusion $\sigma_X = 0.8$, the mixing rate is $\overline{D} = 2.7$.

2. Model forcing

We demonstrate an example in Fig. 4 with a nonuniform spatial mean, by forcing the three most energetic shear modes, for a regime with a small constant mean sweep and small tracer particle diffusion. The model forcing generates a coherent jetlike flow. Forcing does not impact the dispersion rate compared to unforced models. The main observation is the large preconstant at short times, which is due to the jet and the uniform distribution of the particles at $t = 0$.

3. Spectral slope

In the examples in Figs. 5 and 6, we compare varying the spectral slope (shear energy) of the model for regimes with a small constant mean sweep, small tracer particle diffusion, and no background mean rotation term. A more energetic spectrum leads to more violent velocity fields and the tracer trajectories are thus more energetic with larger mixing rates compared to cases with steeper spectra, where the energy of the smallest scales is comparatively

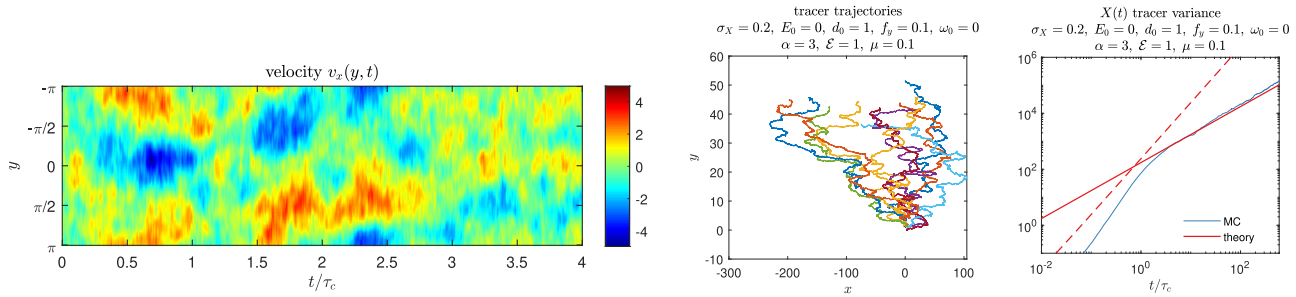

FIG. 5. Example where the shear satisfies the power law spectrum with $E_k \propto |k|^{-3}$. Left pane plots the shear term $u(y, t)$, middle pane plots the tracer particle trajectories, and the right pane plots the tracer variance $\sigma_X^2(t)$.

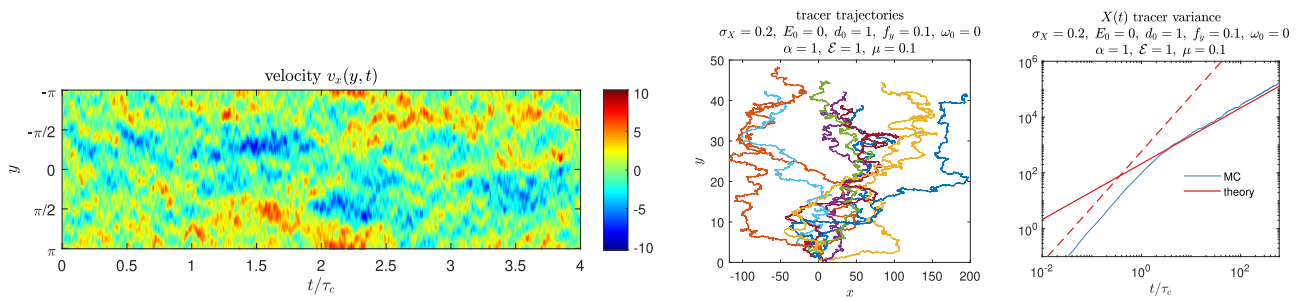

FIG. 6. Example where the shear satisfies the power law spectrum with $E_k \propto |k|^{-1}$. Left pane plots the shear term $u(y, t)$, middle pane plots the tracer particle trajectories, and the right pane plots the tracer variance $\sigma_X^2(t)$.

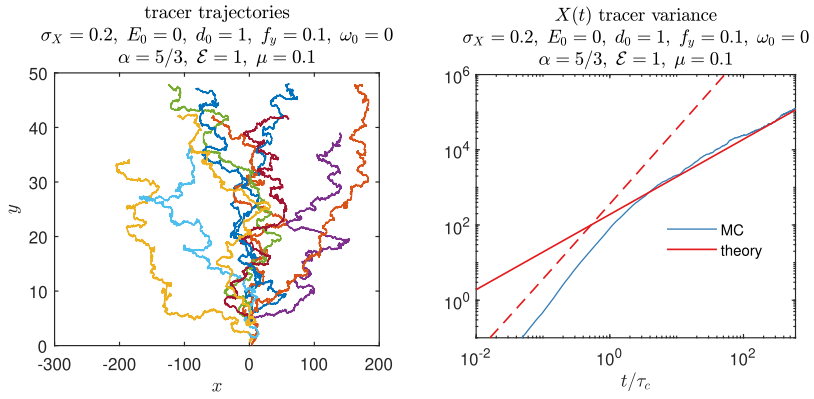

FIG. 7. Example where the cross-sweep magnitude is $\overline{w}_y = 0.1$. Tracer particle trajectories are plotted in the left pane and the tracer variance $\sigma_X^2(t)$ in the right pane.

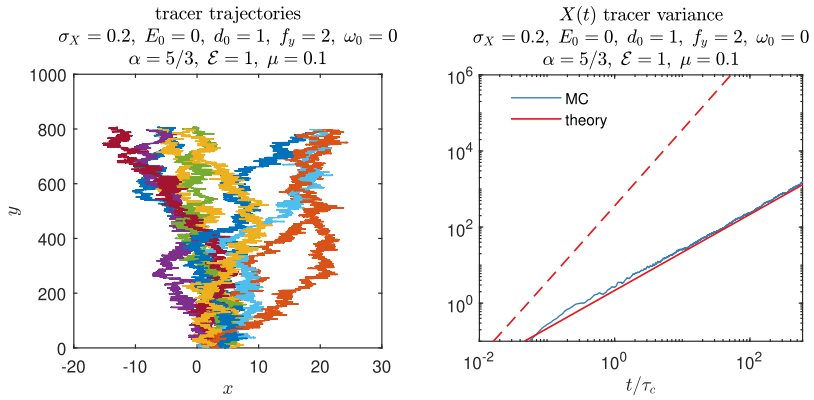

FIG. 8. Example where the cross-sweep magnitude is $\overline{w}_y = 2$. Tracer particle trajectories are plotted in the left pane and the tracer variance $\sigma_X^2(t)$ in the right pane.

weaker. However, the differences between these two examples are not as pronounced since the dependence on the mixing rate for large wavenumbers is reduced at long times [see Eq. (71)]. The short time behavior is more greatly impacted by the spectral slope [see Eq. (68)], especially for small magnitudes of molecular diffusivity.

4. Constant background mean magnitude

For the examples in Figs. 7 and 8, the constant mean sweep strength is varied for regimes with small particle diffusion magnitudes. We see how a strong mean impedes dispersion since the effects of the shear on tracer particles is greatly reduced. In particular, note the scale of the vertical and horizontal axes. The strong vertical mean example with $\overline{w}_y = 2$ results in particles looping around a periodic box 20 times more than when $\overline{w}_y = 0.1$. In addition, particles under the strong mean example are trapped and have a restricted horizontal extent, which results in reduced dispersion rates along the shear.

5. Random background mean

We now include examples of velocity models with a random background mean, which introduces new physical features. Compare Figs. 9 and 10, where we see that a highly energetic mean E_0

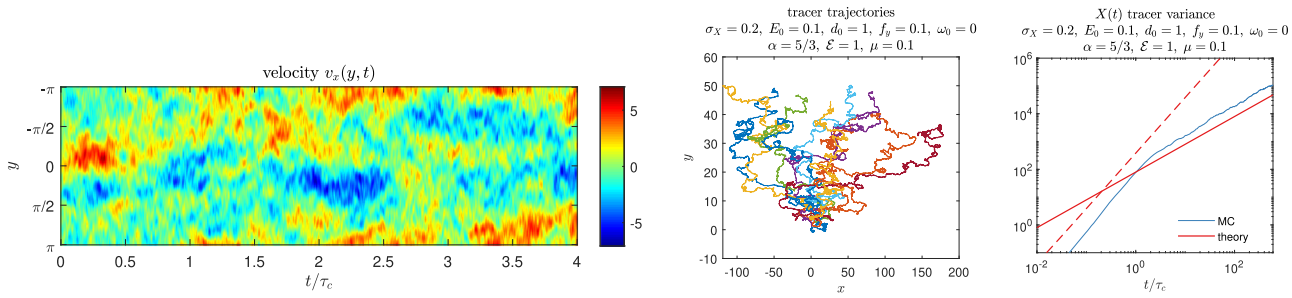

FIG. 9. Example where the background mean has parameters $E_0 = 0.1$, $d_0 = 1$, and $\omega_0 = 0$. Left pane plots the shear term $u(y, t)$, middle pane plots tracer particle trajectories, and the right pane plots the tracer variance $\sigma_X^2(t)$.

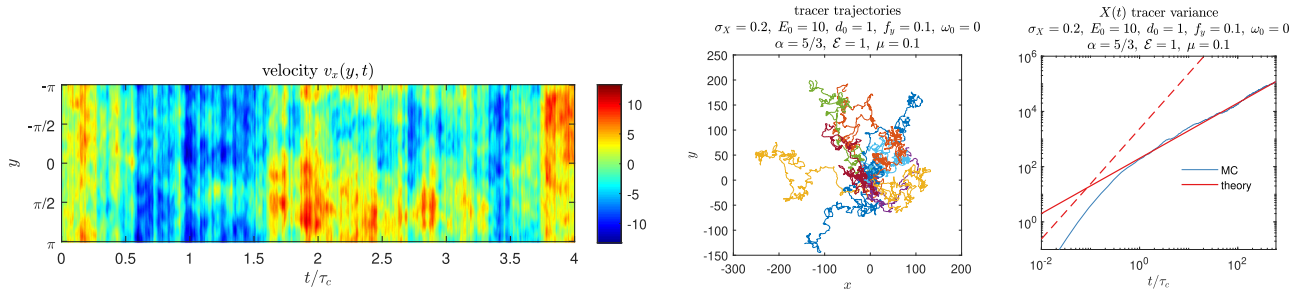

FIG. 10. Example where the background mean has parameters E_0 = 1, d_0 = 1, and ω_0 = 0. Left pane plots the shear term $u(y, t)$, middle pane plots tracer particle trajectories, and the right pane plots the tracer variance $\sigma_X^2(t)$.

results in prominent vertical striations in the Eulerian velocity field. As discussed in Sec. VIII C, an energetic background impedes tracers from advection along the shear and reduces the overall mixing rate, as observed in these test examples.

In Figs. 9 and 11, we fix the background energy level E_0 and show the effects of varying the time scale of the background fluctuations by changing the mean damping d_0. Observe how large damping values (short time correlations) results in increased mixing rates, since then the mean fluctuations act on very short time scales, which effectively diminishes the effects that a highly energetic mean has on reducing dispersion rates. Conversely, observe how small damping (long time correlations) acts to suppress mixing.

Figure 12 demonstrates an example with strong rotation ω_0. Observe that an oscillating background mean results in greater mixing compared to the conditions with zero rotation in the example in Fig. 9, even though in both cases the mean has equivalent energy. As mentioned in Sec. VIII C, rotation results in particles meandering along the shear and the resulting behavior counteracts the noise in the mean, which tries to prevent the particles from dispersing along the shear direction.

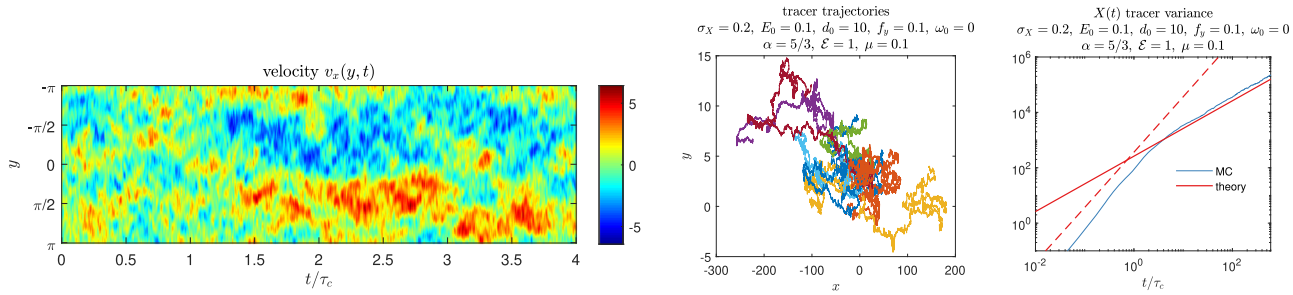

FIG. 11. Example where the background mean has parameters E_0 = 0.1, d_0 = 10, and ω_0 = 0. Left pane plots the shear term $u(y, t)$, middle pane plots tracer particle trajectories, and the right pane plots the tracer variance $\sigma_X^2(t)$.

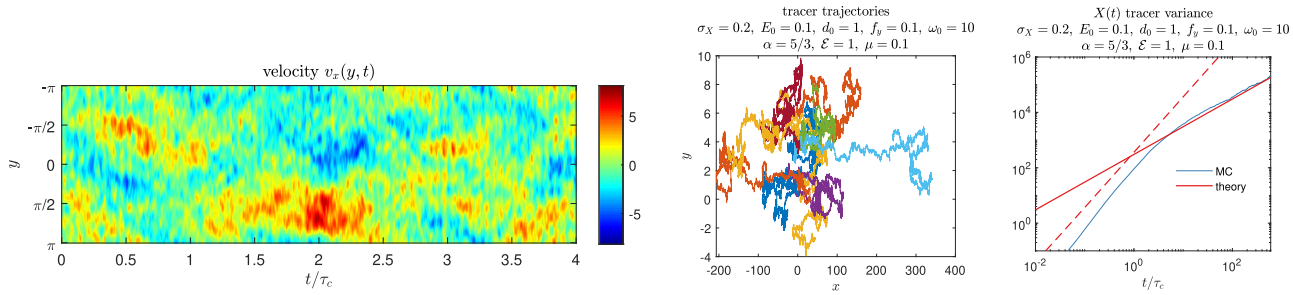

FIG. 12. Example where the background mean has parameters E_0 = 0.1, d_0 = 1, and ω_0 = 10. Left pane plots the shear term $u(y, t)$, middle pane plots tracer particle trajectories, and the right pane plots the tracer variance $\sigma_X^2(t)$.

X. CONCLUSIONS

Here, we studied passively advected Lagrangian particles in a stochastic turbulent shear model, consisting of a randomly fluctuating spatial mean superimposed with a random shear component. The proposed model is rich enough to highlight important differences in the Eulerian vs Lagrangian perspective that arise in more general flows. At the same time, the model is simple enough to admit exactly solvable statistics and thus serves as an important test problem for Lagrangian data assimilation and parameter estimation algorithms. An important element of the turbulent shear model is that it included a nondeterministic mean and a nontrivial shear term that interact to determine the tracer transport rates. We demonstrated how the cross-sweep component of the mean interacts with the shear components in terms of tracer dispersion rates. We directly solved for both the Eulerian and Lagrangian velocity statistics for such simplified velocity models. We also derived theoretical predictions for the mean-square particle displacements in the long and short time asymptotic limits. Then, we compared and highlighted the differences between the Eulerian and Lagrangian perspective for this special model. We discussed how each model parameter effects Lagrangian particle advection and demonstrated accuracy of our derived formulas for the mixing rate with numerical comparisons. The numerical model regime studies complemented the physical description of each model term and demonstrated particle behavior and their extent in space and time. Future work utilizes the proposed model for combined filtering and parameter estimation of the turbulent Eulerian velocity spectrum, which is a broadly important problem in atmospheric and ocean science and in engineering. It would be beneficial to study inertial effects for the models considered in this work using simplified frameworks that account for the finite mass of real particles.[42,43]

ACKNOWLEDGMENTS

A.J.M. acknowledges partial support from the Office of Naval Research through Grant No. N00014-19-S-B001. M.A.M. was supported as a postdoctoral fellow on the same grant.

APPENDIX A: NOMENCLATURE AND NOTATION

We define the nomenclature used through the work as follows:

- Vectors in bold italic notation, such as $\boldsymbol{X}, \boldsymbol{x}$
- Matrices in upright, uppercase nonbold notation, e.g., Ω, Λ, Σ.
- Components of a vector by $\boldsymbol{a} = (a_1, a_2, a_3)$.
- Standard basis function in Euclidean space $\mathbf{e}_x, \mathbf{e}_y, \mathbf{e}_z$.
- Complex conjugate of a complex valued variable a by a^*.
- Hermitian transpose of matrix A by A^* or vector $\boldsymbol{a}$ by $\boldsymbol{a}^*$.
- Correlation function of a stochastic process $x(t)$ by $R_x(t_1, t_2)$ or for a stationary process $R_x(\tau)$.
- Statistical (ensemble) mean of a stochastic process by $\langle\cdot\rangle$, e.g., for a variable x, we write $\overline{x} \equiv \langle x \rangle$.
- Fluctuations of a stochastic process x about its statistical mean by $\tilde{x} = x - \overline{x}$.
- Velocity field $\boldsymbol{v} = (v_x, v_y)$.
- Spatial mean of a velocity field $\boldsymbol{v}(\boldsymbol{x}, t)$ by $\boldsymbol{w}(t)$.
- Eulerian velocity by $\boldsymbol{v}(\boldsymbol{x}, t)$ and Lagrangian velocity by $\boldsymbol{v}^{\mathsf{L}}(\boldsymbol{x}, t)$.
- The notation $R_{\boldsymbol{v}}(\boldsymbol{x}, t)$ is used to denote the Eulerian correlation function of a stationary field $\boldsymbol{v}(\boldsymbol{x}, t)$.
- Lagrangian pair correlation function $R^{\mathsf{L}_2}_{\boldsymbol{v}}(\boldsymbol{x}, t)$ of a stationary field $\boldsymbol{v}(\boldsymbol{x}, t)$.
- Lagrangian autocorrelation function $R^{\mathsf{L}}_{\boldsymbol{v}}(t) \equiv R^{\mathsf{L}_2}_{\boldsymbol{v}}(0, t)$ of a stationary field $\boldsymbol{v}(\boldsymbol{x}, t)$.

APPENDIX B: SOLUTION AND STATISTICAL PROPERTIES OF THE VELOCITY MODEL

The following results are standard and can also be found in Refs. 44 and 45.

1. Statistics of the spatially uniform background mean

The analytical solution of the background velocity field,

$$d\boldsymbol{w}(t) = \big((-\Gamma_0 + \Omega_0)\boldsymbol{w}(t) + \boldsymbol{f}_0\big)\,dt + \Sigma_0\,d\boldsymbol{W}_0(t), \tag{B1}$$

may be solved by an integrating factor. With initial condition $\boldsymbol{w}(0) = \boldsymbol{w}_0 = (w_{0x}, w_{0y})$, define $A = -\Gamma_0 + \Omega_0$, and then

$$\boldsymbol{w}(t) = e^{At}\boldsymbol{w}_0 + \int_0^t e^{A(t-s)}\boldsymbol{f}_0(s)\,ds + \int_0^t e^{A(t-s)}\Sigma_0\,d\boldsymbol{W}_0(s). \tag{B2}$$

A simpler way to proceed is by adopting the complex variable approach. The dissipation matrix Γ_0, the skew symmetric rotation matrix Σ_0, and the diffusion matrix Σ_0 are explicitly

$$\Gamma_0 = \begin{pmatrix} d_0 & 0 \\ 0 & d_0 \end{pmatrix}, \quad \Omega_0 = \begin{pmatrix} 0 & -\omega_0 \\ \omega_0 & 0 \end{pmatrix}, \quad \Sigma_0 = \begin{pmatrix} \sigma_0 & 0 \\ 0 & \sigma_0 \end{pmatrix}. \tag{B3}$$

These 2×2 matrices can be represented by complex numbers. Hence, we can represent the velocity $\boldsymbol{w} = (w_x, w_y)$ as a complex variable $w = w_x + iw_y$, satisfying

$$dw(t) = \big((-d_0 + i\omega_0)w(t) + f_0\big)\,dt + \sqrt{2}\sigma_0\,dW_0(t), \tag{B4}$$

where $f_0 = f_{0x} + if_{0y}$, with $\boldsymbol{f}_0 = (f_{0x}, f_{0y})$. Define $p_0 = -d_0 + i\omega_0$, and the solution of this complex Ornstein-Uhlenbeck process is given by

$$w(t) = e^{p_0 t}w_0 - \frac{f_0}{p_0}(1 - e^{pt}) + \sqrt{2}\sigma_0 \int_0^t e^{p_0(t-s)}\,dW(s), \tag{B5}$$

where $w_0 = w_{0x} + iw_{0y}$. Assuming a constant initial condition, the mean and variance of this process are

$$\overline{w}(t) = e^{p_0 t}w_0 - \frac{f_0}{p_0}(1 - e^{p_0 t}) = -\frac{f_0}{p_0} + e^{p_0 t}\Big(w_0 + \frac{f_0}{p_0}\Big), \tag{B6}$$

$$\mathrm{Var}(w(t)) = \frac{\sigma_0^2}{d_0}(1 - e^{-2d_0 t}), \tag{B7}$$

and hence asymptotically $w(t) \sim N(-\frac{f_0}{p_0}, \frac{\sigma_0^2}{d_0})$ or always if $w_0 \sim N(-\frac{f_0}{p_0}, \frac{\sigma_0^2}{d_0})$. Furthermore, the temporal autocorrelation function can also be shown to be

$$\begin{aligned} R_w(t, t') &= \big\langle (w(t) - \overline{w}(t))(w(t') - \overline{w}(t'))^* \big\rangle \\ &= \frac{\sigma_0^2}{d_0} e^{d_0(t-t') - i w_0 (t'-t)}(1 - e^{-2d_0 t}) \end{aligned} \tag{B8}$$

and in the asymptotic regime by

$$R_w(\tau) = \frac{\sigma_0^2}{d_0} e^{(-d_0 - i\omega_0)\tau}. \tag{B9}$$

2. Statistics of the modal coefficients of the shear term

Each Fourier mode also satisfies a complex Ornstein-Uhlenbeck process, and repeating the calculations from Appendix B 1 shows that the solution of

$$da_k(t) = \left(p_k a_k(t) + f_k\right) dt + \sigma_k \, dW_k(t), \tag{B10}$$

where $p_k = -d_k + i\omega_k$, with initial conditions $a_k(0) = a_{k0}$, is given by

$$a_k = e^{p_k t} a_{k0} - \frac{f_k}{p_k}(1 - e^{p_k t}) + \sigma_k \int_0^t e^{p_k (t-s)} \, dW(s), \tag{B11}$$

with mean and variance, respectively,

$$\overline{a_k}(t) = e^{p_k t} a_{k0} - \frac{f_k}{p_k}(1 - e^{p_k t}) = -\frac{f_k}{p_k} + e^{p_k t}\left(a_{k0} + \frac{f_k}{p_k}\right) \tag{B12}$$

$$\mathrm{Var}(a_k(t)) = \frac{\sigma_k^2}{2d_k}(1 - e^{-2d_k t}), \tag{B13}$$

and hence asymptotically $a_k \sim N(-\frac{f_k}{p_k}, \frac{\sigma_k^2}{2d_k})$ or always if $a_{k0} \sim N(-\frac{f_k}{p_k}, \frac{\sigma_k^2}{2d_k})$. The autocorrelation function in the asymptotic regime can be shown to be given by

$$R_{a_k}(\tau) = \frac{\sigma_k^2}{2d_k} e^{(-d_k - i\omega_k)\tau}. \tag{B14}$$

REFERENCES

[1] T. Rossby, in *Lagrangian Analysis and Prediction of Coastal and Ocean Dynamics*, edited by A. Griffa, A. D. Kirwan, Jr., A. J. Mariano, T. Özgökmen, and H. T. Rossby (Cambridge University Press, 2007), pp. 1–38.

[2] R. Lumpkin and M. Pazos, in *Lagrangian Analysis and Prediction of Coastal and Ocean Dynamics*, edited by A. Griffa, A. D. Kirwan, Jr., A. J. Mariano, T. Özgökmen, and H. T. Rossby (Cambridge University Press, 2007), pp. 39–67.

[3] J. C. Weil, R. I. Sykes, and A. Venkatram, "Evaluating air-quality models: Review and outlook," J. Appl. Meteorol. **31**, 1121–1145 (1992).

[4] Q. A. Wang, "Probability distribution and entropy as a measure of uncertainty," J. Phys. A: Math. Theor. **41**, 065004 (2008).

[5] C. Celis and L. F. Figueira da Silva, "Lagrangian mixing models for turbulent combustion: Review and prospects," Flow, Turbul. Combust. **94**, 643–689 (2015).

[6] M. Holzner, A. Liberzon, N. Nikitin, B. Lüthi, W. Kinzelbach, and A. Tsinober, "A Lagrangian investigation of the small-scale features of turbulent entrainment through particle tracking and direct numerical simulation," J. Fluid Mech. **598**, 465–475 (2008).

[7] P. K. Yeung, "Lagrangian investigations of turbulence," Annu. Rev. Fluid Mech. **34**, 115–142 (2002).

[8] S. B. Pope, *Turbulent Flows*, 1st ed. (Cambridge University Press, 2000).

[9] F. Toschi and E. Bodenschatz, "Lagrangian properties of particles in turbulence," Annu. Rev. Fluid Mech. **41**, 375–404 (2009).

[10] G. I. Taylor, "The spectrum of turbulence," Proc. R. Soc. London, Ser. A **164**, 476–490 (1938).

[11] G. I. Taylor, "Diffusion by continuous movements," Proc. London Math. Soc. **s2-20**, 196–212 (1922).

[12] G. K. Batchelor, "Diffusion in free turbulent shear flows," J. Fluid Mech. **3**, 67–80 (1957).

[13] G. K. Batchelor, "The application of the similarity theory of turbulence to atmospheric diffusion," Q. J. R. Metereol. Soc. **76**, 133–146 (1950).

[14] L. F. Richardson, "Atmospheric diffusion shown on a distance-neighbour graph," Proc. R. Soc. London, Ser. A **110**, 709–737 (1926).

[15] A. F. Bennett, "A Lagrangian analysis of turbulent diffusion," Rev. Geophys. **25**, 799–822, https://doi.org/10.1029/rg025i004p00799 (1987).

[16] A. Bennett, *Lagrangian Fluid Dynamics* (Cambridge University Press, 2006).

[17] J. H. LaCasce, "Statistics from Lagrangian observations," Prog. Oceanogr. **77**, 1–29 (2008).

[18] B. Sawford, "Turbulent relative dispersion," Annu. Rev. Fluid Mech. **33**, 289–317 (2001).

[19] J. P. L. C. Salazar and L. R. Collins, "Two-particle dispersion in isotropic turbulent flows," Annu. Rev. Fluid Mech. **41**, 405–432 (2009).

[20] D. Buaria, B. L. Sawford, and P. K. Yeung, "Characteristics of backward and forward two-particle relative dispersion in turbulence at different Reynolds numbers," Phys. Fluids **27**, 105101 (2015).

[21] B. L. Sawford, P. K. Yeung, and M. S. Borgas, "Comparison of backwards and forwards relative dispersion in turbulence," Phys. Fluids **17**, 095109 (2005).

[22] J. M. Lilly, A. M. Sykulski, J. J. Early, and S. C. Olhede, "Fractional brownian motion, the Matérn process and stochastic modeling of turbulent dispersion," Nonlinear Processes Geophys. **24**, 481–514 (2017).

[23] B. L. Sawford, S. B. Pope, and P. K. Yeung, "Gaussian Lagrangian stochastic models for multi-particle dispersion," Phys. Fluids **25**, 055101 (2013).

[24] S. P. Blomberg, S. Rathnayake, and C. Moreau, "Beyond Brownian motion and the Ornstein-Uhlenbeck process: Stochastic diffusion models for the evolution of quantitative characters," Am. Nat. (to be published) bioRxiv: 067363 (2019).

[25] D. Balwada, J. H. LaCasce, and K. G. Speer, "Scale-dependent distribution of kinetic energy from surface drifters in the Gulf of Mexico," Geophys. Res. Lett. **43**, 10856–10863, https://doi.org/10.1002/2016gl069405 (2016).

[26] F. J. Beron-Vera and J. H. LaCasce, "Statistics of simulated and observed pair separations in the Gulf of Mexico," J. Phys. Oceanogr. **46**, 2183–2199 (2016).

[27] C. J. Roach, D. Balwada, and K. Speer, "Global observations of horizontal mixing from argo float and surface drifter trajectories," J. Geophys. Res.: Oceans **123**, 4560–4575, https://doi.org/10.1029/2018jc013750 (2018).

[28] W. R. Young, P. B. Rhines, and C. J. R. Garrett, "Shear-flow dispersion, internal waves and horizontal mixing in the ocean," J. Phys. Oceanogr. **12**, 515–527 (1982).

[29] A. J. Majda and B. Gershgorin, "Elementary models for turbulent diffusion with complex physical features: Eddy diffusivity, spectrum and intermittency," Philos. Trans. R. Soc., A **371**, 20120184 (2013).

[30] A. J. Majda and P. R. Kramer, "Simplified models for turbulent diffusion: Theory, numerical modelling, and physical phenomena," Phys. Rep. **314**, 237–574 (1999).

[31] A. J. Majda and X. T. Tong, "Intermittency in turbulent diffusion models with a mean gradient," Nonlinearity **28**, 4171 (2015).

[32] A. J. Majda and R. M. McLaughlin, "The effect of mean flows on enhanced diffusivity in transport by incompressible periodic velocity fields," Stud. Appl. Math. **89**, 245–279 (1993).

[33] M. A. Mohamad, W. Cousins, and T. P. Sapsis, "A probabilistic decomposition-synthesis method for the quantification of rare events due to internal instabilities," J. Comput. Phys. **322**, 288–308 (2016).

[34] N. Chen and A. J. Majda, "Conditional Gaussian systems for multiscale nonlinear stochastic systems: Prediction, state estimation and uncertainty quantification," Entropy **20**, 509 (2018).

[35] R. S. Liptser and A. N. Shiryaev, *Statistics of Random Processes II: Applications*, 2nd ed., Stochastic Modelling and Applied Probability Vol. 6 (Springer-Verlag Berlin Heidelberg, 2001).

[36] A. Apte, C. K. R. T. Jones, and A. M. Stuart, "A Bayesian approach to Lagrangian data assimilation," Tellus A: Dyn. Meteorol. Oceanogr. **60**, 336–347 (2008).

[37] A. Molcard, T. M. Özgökmen, A. Griffa, L. I. Piterbarg, and T. M. Chin, in *Lagrangian Analysis and Prediction of Coastal and Ocean Dynamics*, edited by A. Griffa, A. D. Kirwan, Jr., A. J. Mariano, T. Özgökmen, and H. T. Rossby (Cambridge University Press, 2007), pp. 172–203.

[38]Y. A. Kuznetsov, *Elements of Applied Bifurcation Theory* 3rd ed., Applied Mathematical Sciences Vol. 112 (Springer-Verlag, New York, 2004).
[39]L. Kuznetsov, K. Ide, and C. K. R. T. Jones, "A method for assimilation of Lagrangian data," Mon. Weather Rev. **131**, 2247–2260 (2003).
[40]M. A. Mohamad and A. J. Majda, "Recovering the Eulerian energy spectrum from noisy Lagrangian tracers," Physica D (to be published).
[41]N. Chen, A. J. Majda, and X. T. Tong, "Information barriers for noisy Lagrangian tracers in filtering random incompressible flows," Nonlinearity **27**, 2133 (2014).
[42]F. J. Beron-Vera, M. J. Olascoaga, and P. Miron, "Building a Maxey–Riley framework for surface ocean inertial particle dynamics," Phys. Fluids **31**, 096602 (2019).
[43]M. R. Maxey and J. J. Riley, "Equation of motion for a small rigid sphere in a nonuniform flow," Phys. Fluids **26**, 883–889 (1983).
[44]A. J. Majda and J. Harlim, *Filtering Complex Turbulent Systems* (Cambridge University Press, 2012).
[45]G. A. Pavliotis, *Stochastic Processes and Applications: Diffusion Processes*, The Fokker-Planck and Langevin Equations Texts in Applied Mathematics Vol. 60 (Springer-Verlag New York, 2014).